Quantum and Semiclassical Optics: Journal of the European Optical Society Part B

$\chi^{(2)}$ cascading: nonlinear phase shifts

To cite this article: George I Stegeman 1997 *Quantum Semiclass. Opt.* **9** 139

Quantum Semiclass. Opt. **9** (1997) 139–153. Printed in the UK PII: S1355-5111(97)78890-0

$\chi^{(2)}$ cascading: nonlinear phase shifts

George I Stegeman
Center for Research and Education in Optics and Lasers (CREOL) and Department of Physics, University of Central Florida, 4000 Central Florida Blvd, CREOL Bld., PO Box 162700, Orlando, FL 32816-2700, USA

Received 14 October 1996, in final form 9 December 1996

Abstract. Nonlinear phase shifts which increase with input irradiance can be generated in quadratically nonlinear materials by the exchange of energy between a fundamental and a second harmonic. Here we review this effect, theory and experiment.

1. Introduction

For the first 25 years of nonlinear optics, the phenomena in which the nonlinear polarization is proportional to even or odd powers of the incident optical fields have essentially developed separately. Traditionally, second-order susceptibilities have been utilized for second harmonic generation (SHG), optical parametric oscillators and amplifiers, etc. However, it was recognized in the very early days of nonlinear optics that the periodic energy exchange between waves interacting via $\chi^{(2)}$ in non-phase-matched situations leads to an additional nonlinear phase shift in the fundamental wave [1]. This phase shift can also be interpreted as an effective third-order nonlinearity, but with symmetry and cross-phase modulation properties quite different from those associated with the traditional $\chi^{(3)}$ characteristics. However, $\chi^{(2)}$s were small at that time, at most a few pm V^{-1}. Although interference effects between second- and third-order nonlinearities were reported, away from any resonances the contributions to the nonlinear phase shifts generated via $\chi^{(3)}$ were dominant [2]. Although these phase shifts were considered in various theoretical papers over the next 20 or more years, it was not until 1988 that the nonlinear phase changes were measured experimentally and a large phase shift was reported [3–5]. The phenomenon was highlighted in a paper on Z-scan in KTP in which the cascaded nonlinear phase shift was dominant, and this result revived interest [5].

Such a phase shift or effective third-order nonlinearity has a number of potential applications, some of which have already been investigated. For example, mode-locking of lasers, pulse compression, all-optical waveguide switching, optical bistability, degenerate three-wave mixing, optical transistor action and spatial non-reciprocity have all been reported in the last five years [6–12]. Furthermore, an effective third-order nonlinearity also occurs when down-conversion, i.e. optical rectification, occurs first followed by up-conversion, an effect also predicted in the early years of nonlinear optics [13]. Recently, this effect has also been revisited in the context of Z-scan and four-wave mixing which produced enhanced nonlinearities [14, 15]. In a separate development, spatial solitons based on quadratic nonlinearities, first predicted back in the 1970s, have recently been observed [16, 17].

In this short review we will focus on the properties of cascaded nonlinear phase shifts during harmonic generation, the most widely studied case to date. Consider SHG in which only a single fundamental wave is launched. The fundamental beam (amplitude a_1) inside the medium is given by

$$E = \tfrac{1}{2}|a_1(z)|\sqrt{\frac{2}{cn\epsilon_0}}\exp[\mathrm{i}(\omega t - kz - \phi^{\mathrm{NL}}(z))] + \mathrm{CC}\,. \tag{1}$$

The cascaded phase shift referred to here is $\phi^{\mathrm{NL}}(z)$. Furthermore, the dependence of this phase shift on the distance into the medium, input irradiance, detuning from phase-matching, number of interacting fundamental beams, bandwidth, etc, are all different from the same phenomena with a $\chi^{(3)}$ origin. Finally, we will discuss experimental measurements of ϕ^{NL}.

2. The nonlinear phase shift via SHG: type I

2.1. Governing equations

We start with the usual expansion for the nonlinear polarization when two waves are present, one at the fundamental (ω) and one at the second harmonic (2ω) frequency. Other frequencies, for example the third harmonic, can obviously be generated, but will be neglected for our purposes. The fields are written as

$$\boldsymbol{E}_i(z,t) = \tfrac{1}{2}\boldsymbol{e}_i a_i(z)\sqrt{\frac{2}{cn\epsilon_0}}\exp[\mathrm{i}(\omega_i t - k_i z)] + \mathrm{CC} \tag{2}$$

where $i = 1, 3$ refer to the fundamental and harmonic, respectively, with unit vectors $\boldsymbol{e}_i$. Note that the normalization is chosen so that $|a_1(z)|^2 = I_1(z)$ and $|a_3(z)|^2 = I_3(z)$ are the respective irradiances. We are interested in both the harmonic generation process, and for comparison, the third-order term that leads to the irradiance-dependent refractive index coefficient. The appropriate nonlinear polarization field is given by [18]

$$\begin{aligned} P^{\mathrm{NL}}(z,t) = \frac{1}{2}\Bigg[& \frac{2}{cn_1} d_{\mathrm{eff}}^{(2)}(-2\omega;\omega,\omega)\, a_1^2(z)\, \mathrm{e}^{2\mathrm{i}[\omega t - k_1 z]} \\ & + \frac{4}{c\sqrt{n_1 n_3}} d_{\mathrm{eff}}^{(2)}(-\omega; 2\omega, -\omega)\, a_3(z)\, a_1^*(z)\, \mathrm{e}^{\mathrm{i}(\omega t - [k_3 - k_1]z)} \\ & + \frac{3\sqrt{2^3}}{\sqrt{c^3 n_1^3 \epsilon_0}} \chi_{\mathrm{eff}}^{(3)}(-\omega;\omega,-\omega,\omega)\, |a_1(z)|^2\, a_1(z)\, \mathrm{e}^{\mathrm{i}[\omega t - k_1 z]} + \mathrm{CC}\Bigg] \end{aligned} \tag{3}$$

where the first, second and third terms lead to the up-conversion to the second harmonic, the down-conversion back to the fundamental and the irradiance-dependent refractive index effects, respectively.

The coupled mode equations are now derived in the usual slowly varying phase and amplitude approximation. In the absence of loss they are

$$\frac{\mathrm{d}}{\mathrm{d}z}a_1(z) = -\mathrm{i}\kappa(-\omega; 2\omega, -\omega)\, a_3(z)\, a_1^*(z)\, \mathrm{e}^{\mathrm{i}\Delta kz} - \mathrm{i}\frac{3\omega}{(cn)^2\epsilon_0}\chi_{\mathrm{eff}}^{(3)}|a_1(z)|^2\, a_1(z) \tag{4}$$

$$\frac{\mathrm{d}}{\mathrm{d}z}a_3(z) = -\mathrm{i}\kappa(-2\omega;\omega,\omega)\, a_1^2(z)\, \mathrm{e}^{-\mathrm{i}\Delta kz} \tag{5}$$

$$\kappa(-2\omega;\omega,\omega) = \frac{\omega d_{ijk}^{(2)}(-2\omega;\omega,\omega)\, e_i(2\omega)\, e_j(\omega)\, e_k(\omega)}{[2n_i(2\omega)\, n_j(\omega)\, n_k(\omega)\, c^3\epsilon_0]^{1/2}} \tag{6}$$

$$\kappa(-\omega; 2\omega, -\omega) = \frac{\omega d_{ijk}^{(2)}(-\omega; 2\omega, -\omega)\, e_i(\omega)\, e_j(2\omega)\, e_k(\omega)}{[2n_i(\omega)\, n_j(2\omega)\, n_k(\omega)\, c^3\epsilon_0]^{1/2}} \tag{7}$$

for uniform wavevector mismatch $\Delta k = 2k_1 - k_3 = 2k_{\mathrm{vac}}(\omega)[n_1 - n_3]$.

Whenever full permutation symmetry is valid, $\kappa(-2\omega; \omega, \omega) = \kappa(-\omega; 2\omega, -\omega) = \kappa$ is the nonlinear coupling coefficient. These coupled mode equations for SHG already contain all the information needed to calculate the complex fundamental and harmonic amplitudes as a function of the distance into a crystal, including the nonlinear phase shifts.

2.2. Weak depletion limit

We first investigate the SHG process in the limit of weak SHG and negligible depletion of the fundamental. Solving for the harmonic gives

$$a_2(z) = \frac{\kappa a_1^2(z)}{\Delta k}\left[\mathrm{e}^{\mathrm{i}\Delta k z} - 1\right] \tag{8}$$

and substituting back into equation (4) gives for the SHG related terms

$$\frac{\mathrm{d}}{\mathrm{d}z} a_1(z) = -\mathrm{i}\frac{\kappa^2}{\Delta k}[(1 - \cos(\Delta k z)) - \mathrm{i}\sin(\Delta k z)]|a_1(z)|^2\, a_1(z)\,. \tag{9}$$

We compare this expression with the third-order term, namely

$$\frac{\mathrm{d}}{\mathrm{d}z} a_1(z) = -\mathrm{i}\frac{3\omega}{(cn)^2\epsilon_0}\chi_{\mathrm{eff}}^{(3)}|a_1(z)|^2\, a_1(z)\,. \tag{10}$$

Therefore, in this limit the cascading process mimics a third-order nonlinearity. In terms of an effective irradiance-dependent refractive index coefficient,

$$n_{2,\mathrm{eff}}(z) = \frac{2\pi\left[d_{\mathrm{eff}}^{(2)}\right]^2}{\epsilon_0 c n^4 \lambda \Delta k}[1 - \cos(\Delta k z)]\,. \tag{11}$$

A distance-dependent effective nonlinearity is significantly different to typical third-order nonlinearities. For large wavevector mismatches, the oscillations are rapid in space and the average value of $n_{2,\,\mathrm{eff}}$ is simply

$$n_{2,\,\mathrm{eff}} = \frac{2\pi\left[d_{\mathrm{eff}}^{(2)}\right]^2}{\epsilon_0 c n^4 \lambda \Delta k} \tag{12}$$

i.e. proportional to Δk^{-1} as noted in the early days of nonlinear optics. Note that in this limit the nonlinearity is maximized from (11) for $\Delta k L = \pm\pi$ for a sample of length L, leading to the result that $n_{2,\,\mathrm{eff}} \propto L$ in this case. Evaluating the maximum value for the effective nonlinearity gives the values quoted in table 1 for a few materials. These values appear to be very promising, especially when compared with the largest known non-resonant third-order nonlinearity, $n_2 = 2.2 \times 10^{-12}$ cm^2 W^{-1} [19]. The key problem to be solved will be to find appropriate phase-matching techniques. Furthermore, if phase shifts of 1–2π are required for a specific application, the effective nonlinearity is significantly degraded because the nonlinear phase shift ϕ^{NL} is no longer proportional to the irradiance, as will be discussed later.

Table 1. Effective, maximum, nonlinear coefficients n_2 achievable with cascading for materials with representative large d_{ij}. NPP, N-(4-nitrophenyl)-(L)-prolinol [20]. MNA, 2-methyl-4-nitroaniline [21]. DAST, dimethyl amino stilbazolium tosylate [22].

Material ($L = 1$ cm)	d_{ii} (pm V^{-1})	d_{ij} (pm V^{-1})	n_2 (effective) (cm^2 W^{-1})
$LiNbO_3$	36		2×10^{-11}
$LiNbO_3$		5.8	5×10^{-13}
MNA	165		7×10^{-10}
NPP		84	2×10^{-10}
DAST	600		6×10^{-9}

2.3. Simple model for the phase shift

How the cascading process leads to a nonlinear phase shift can be understood in terms of the simple physics of type I (single fundamental input beam) SHG. In the non-phase-matched case power is continuously being converted from the fundamental (up-conversion) to the SH, and from the SH to the fundamental (down-conversion). As indicated schematically in figure 1, we simplify the process conceptually so that the up-conversion and down-conversion occur at specific locations separated by one half the coherence length so that after one coherence length the process repeats itself. The thick line represents the fundamental beam and the thin line the second harmonic. The second harmonic is generated at the input via $\omega + \omega \rightarrow 2\omega$. It travels at a different phase velocity v_3 from the fundamental (v_1), assumed here to be $v_3 > v_1$. After typically one half a coherence length, i.e. $L_c = \pi/[2k_{vac}(\omega)|n_1 - n_3|]$, the second harmonic down-converts back to the fundamental, i.e. $2\omega - \omega \rightarrow \omega$. Because the process is not phase-matched, the returning (regenerated) fundamental wave has a different phase from the original fundamental beam that was not converted to SHG. The accumulated phase difference is $\Delta\phi = \phi_1 - \phi_3 > 0$. Note that for $\Delta k < 0$, $\Delta\phi < 0$.

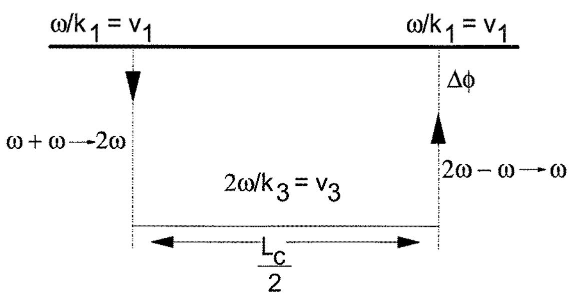

Figure 1. Schematic of the cascading geometry in which a fundamental beam is incident on a $\chi^{(2)}$-active medium near its phase-matching condition and generates a second harmonic.

To understand the sign of the effective nonlinearity and phase shift, it is also necessary to include the π relative phase between the unconverted and regenerated fundamental. It comes directly from two successive applications of the coupled mode equations which give the multiplier $i^2 = -1$. The origin of the π shift is well known. It ensures energy conservation right at phase-matching so that as the second harmonic grows, the regenerated fundamental which is continuously being generated via equation (4) is exactly out of phase with the non-converted fundamental, therefore depleting it.

Figure 2 shows schematically how this π phase shift affects the sign of the effective nonlinearity away from phase-matching. We show the greatly over-simplified situation

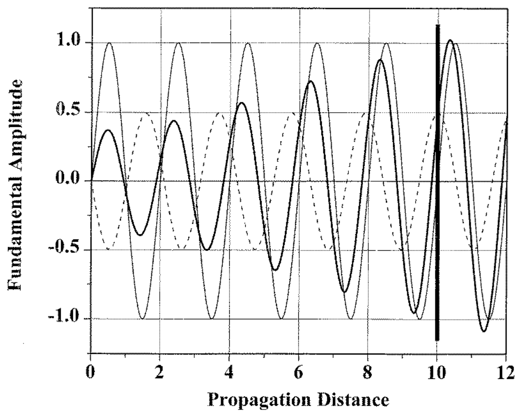

Figure 2. The simplified evolution in space of the unconverted fundamental (constant amplitude, light full curve), the regenerated fundamental (constant amplitude, broken curve) and the total fundamental (heavy full curve). The co-launched fields (unconverted and regenerated fundamentals) are π out of phase at the origin. The full vertical line corresponds to one quarter of a coherence length.

where the regenerated and unconverted fundamental are assumed to have a constant amplitude with distance and are co-launched at the origin π out of phase. (In reality, neither field has a constant amplitude and power exchange occurs continuously with distance.) We also show the sum of the unconverted and regenerated fundamental to indicate the evolution of the nonlinear phase shift for $\Delta k > 0$, i.e. $n_1(\omega) > n_3(\omega)$. The key point is that although the regenerated wave clearly leads the unconverted fundamental, the 'sum' fundamental lags progressively further behind the unconverted fundamental with propagation distance. This corresponds to an effective increase in the refractive index of the 'sum' fundamental. Hence the cascading process effectively leads to an increased refractive index for the fundamental, i.e. $n_{2,\,\mathrm{eff}} > 0$ for $\Delta k > 0$, as given by equations (11) and (12).

The larger the depletion of the fundamental, the more second harmonic is generated, the larger the net fundamental phase shift on down-conversion, reaching a maximum value of $\pi/2$. Because the SHG conversion efficiency depends on the input irradiance and the net phase shift depends on the irradiance of the second harmonic, the resulting phase shift is also 'nonlinear'. This nonlinearity is 'non-local' since it requires some propagation of the second harmonic to occur. Note that either sign for $\Delta\phi$ is possible, depending on whether $n_1 > n_3$, or vice versa. Although this brief explanation has been limited to type I phase-matching, it can easily be extended to type II phase-matching, and in general to other parametric processes.

2.4. Analytical solutions

The seminal paper by Armstrong *et al* in 1962 not only contained the derivation of the fundamental coupled mode equations, but also the general analytical solutions for SHG [23]. A complete analysis of the phase shifts for all cases of interest has been given in terms of Jacobi elliptic integrals by Kobyakov and co-workers [24].

2.5. Numerical examples

Although we have discussed an effective cascaded 'n_2' nonlinearity, the fundamental parameter is actually the nonlinear phase shift. When dealing with third-order effects, $\chi^{(3)}$ is a local material property, whereas in cascading propagation is an integral part of the effect and the phase shift reflects both the material properties and the optical propagation. Researchers using n_2 are accustomed to certain characteristics such as nonlinear phase shifts which are linear with propagation distance and irradiance. In cascading, an approximately linear dependence of ϕ^{NL} on either the distance into the sample or on the incident irradiance (and hence equivalence to $\chi^{(3)}$) can also occur, but only for large phase mismatch (ΔkL) and/or small phase shifts. Detailed examples of the actual variation of $\phi^{\mathrm{NL}}(z)$ with distance are reproduced in figure 3(*a*) [25]. They show:

(i) Stepwise changes in $\phi^{\mathrm{NL}}(z)$ with increasing distance, with a maximum step size of $\pi/2$.

(ii) Even for large phase mismatches the increase occurs via steps, the larger the phase mismatch the smaller (and more frequent) the steps.

(iii) Comparison with the throughput curves (figure 3(*b*)) indicates that the increment (step) in nonlinear phase occurs primarily during the cycle in which power flows back from the harmonic into the fundamental, as predicted by the model discussed above.

The dependence of $\phi^{\mathrm{NL}}(L)$ (i.e. at the output) on the input irradiance is shown in figure 4 [25].

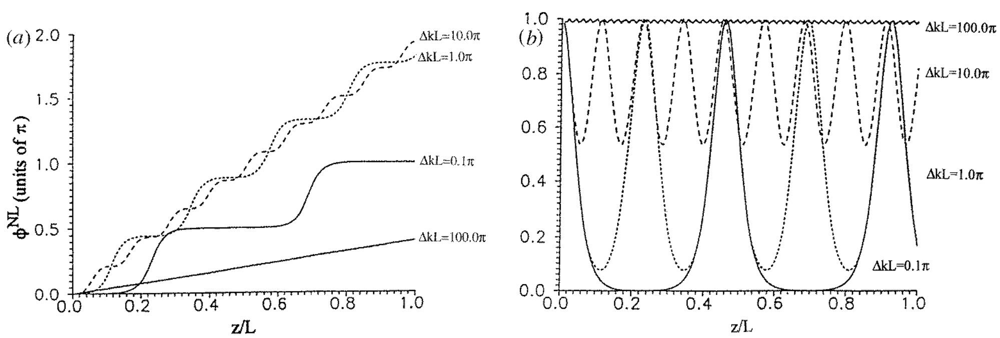

Figure 3. Typical variation of (*a*) the nonlinear phase shift $\phi^{\mathrm{NL}}(z/L)$ and (*b*) the transmitted fundamental with normalized distance z/L for various net phase mismatches ΔkL for type I SHG. Here $\kappa L = 4$ and $|a_1(0)|^2 = 25$ (from [25]).

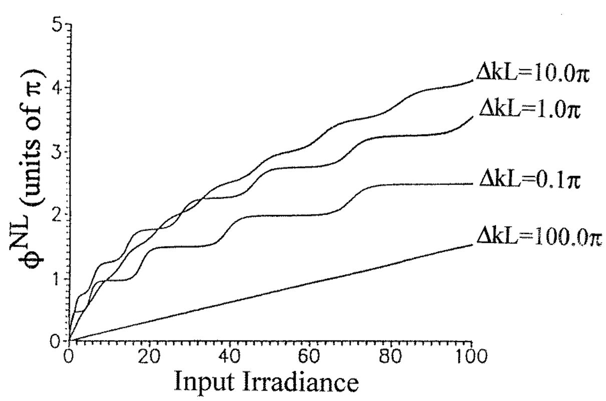

Figure 4. Typical variation in the nonlinear phase shift $\phi^{\mathrm{NL}}(L)$ versus fundamental input irradiance for various net phase mismatches. Here $\kappa L = 4$ (from [25]).

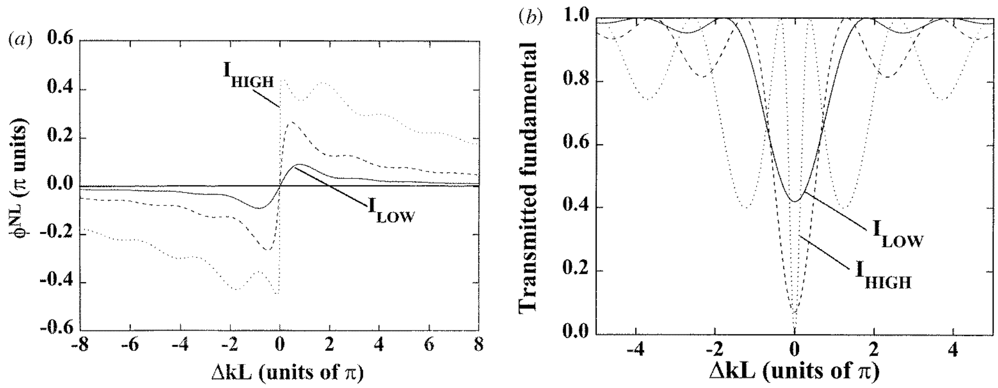

Figure 5. Typical variation in (a) the nonlinear phase shift $\phi^{\mathrm{NL}}(L)$ and (b) the fundamental transmission versus detuning from phase matching ΔkL for three different input irradiances.

(i) It occurs in steps, just like the distance dependence.

(ii) The nonlinear phase shift apparently saturates with increasing irradiance, even after averaging over the steps. In fact, $\phi^{\mathrm{NL}}(L)$ becomes asymptotically linear in the field at large phase shifts, emphasizing the second-order origin of the effect.

As implied by the simple model described above, the sign and magnitude of the net phase shift depend on the details of the phase mismatch, commonly called the SHG detuning. This variation is shown in figure 5(a). Furthermore, there is an irradiance dependence to the detuning needed for maximum phase shift: in the small-depletion limit this maximum occurs at $\Delta kL = \pm\pi$ which increases at higher irradiances. The dispersion in the low-depletion limit is reminiscent of the dispersion with wavelength of refractive index due to the strong energy exchange between an EM field and a two-level transition near resonance: here the corresponding energy exchange is between two electromagnetic modes, the fundamental and second harmonic and the corresponding resonance is the phase-matching condition between the two modes. As shown in figure 5(b), the 'price' for obtaining large phase shifts is effectively the 'loss' of the fundamental throughput to the second harmonic (which effectively acts as the well known two-photon absorption in $\chi^{(3)}$ nonlinear optics). This reduction in fundamental throughput is a serious drawback for cascading. However, because the process is nonlocal, it can be avoided as will be discussed later. Note also the well known effective change in coherence length in figure 5(b) at high input irradiances [23].

2.6. Nonlinear eigenmodes

Eigenmode solutions exist to the SHG coupled mode equations. That is, for a certain combination of fundamental and harmonic input, there is no net power exchange with distance between the fundamental and harmonic fields. This does not exclude changes in phase for the two beams with distance. Trillo and Wabnitz, and Kaplan have shown that this leads to two eigenmodes [26]. They must be launched with both a specific difference between their phases at the input, i.e. $\Delta\phi = (S-1)\pi/2$ with $S = \pm 1$, and with relative wave irradiances given by

$$I_1(z) = 2I_3(z) + S\frac{c\Delta k}{\omega}\sqrt{I_3(z)I_{\max}} \qquad I_{\max} = \frac{n_1\sqrt{cn_3\epsilon_0}}{d_{\mathrm{eff}}^{(2)}}\,. \tag{13}$$

As long as $I_{\max} < 4I_3(z)\,\omega^2/c^2\Delta k^2$, i.e. for small enough wavevector mismatch, there are two solutions. Otherwise, only the $S = +1$ solution exists. The phase shifts are given by $\phi^{\mathrm{NL}}(z) = -S[\omega^2 I_3(z)/(c^2 I_{\max})]^{1/2} z$, and their sign clearly depends on the relative phases at the input. However, note that the phase shift is linear in the field—the asymptotic limit of SHG for very large irradiances.

3. The nonlinear phase shift via SHG: type II

There are more variables and therefore more possibilities for type II phase-matching because there are two, independently controlled, fundamental input beams [24, 27–29]. The additional degree of freedom relative to the type I case is the relative irradiance of the two fundamental inputs. (We note that the relative phase of the two input fundamentals affects neither the conversion efficiency nor the nonlinear phase shifts.) Three coupled mode equations are needed to describe the interaction between the three complex amplitudes $a_1(z)$ (frequency ω, wavevector $\boldsymbol{k}_1$), $a_2(z)$ (frequency ω, wavevector $\boldsymbol{k}_2$) and $a_3(z)$ (frequency 2ω, wavevector $\boldsymbol{k}_3$):

$$\frac{\mathrm{d}}{\mathrm{d}z}a_1(z) = -\mathrm{i}\kappa(-\omega; 2\omega, -\omega)\, a_3(z)\, a_2^*(z)\, \mathrm{e}^{\mathrm{i}\Delta kz} \tag{14}$$

$$\frac{\mathrm{d}}{\mathrm{d}z}a_2(z) = -\mathrm{i}\kappa(-\omega; 2\omega, -\omega)\, a_1^*(z)\, a_3(z)\, \mathrm{e}^{\mathrm{i}\Delta kz} \tag{15}$$

$$\frac{\mathrm{d}}{\mathrm{d}z}a_3(z) = -\mathrm{i}\kappa(-2\omega; \omega, \omega)\, a_1(z)\, a_2(z)\, \mathrm{e}^{-\mathrm{i}\Delta kz} \tag{16}$$

where the wavevector mismatch for collinear beams is given by $\Delta k = [k_1 + k_2 - k_3]$. Again assuming full permutation symmetry reduces the coupling coefficients to a common κ. The irradiances (plane wave) are given by $I_1(z) = |a_1(z)|^2$, $I_2(z) = |a_2(z)|^2$ and $I_3(z) = |a_3(z)|^2$. For SHG, $|a_1(0)|^2 = I_1(0)$, $|a_2(0)|^2 = I_2(0)$ and $|a_3(0)|^2 = 0$.

The most interesting aspect of this type II geometry occurs when the two fundamental inputs are not equal. (The equal irradiance case reduces to the type I response just discussed.) Every conceivable case of interest has been investigated by Lederer and colleagues [24]. In contrast to the type I case, the weaker of the two fundamentals experiences a nonlinear phase shift even right at phase-matching, as shown in figure 6. Furthermore, the irradiance of all

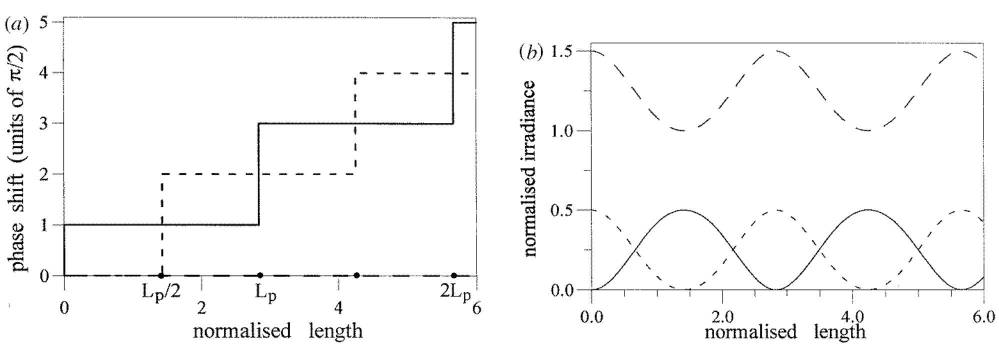

Figure 6. Typical variation at phase-matching in (*a*) the nonlinear phase shift $\phi^{\mathrm{NL}}(z)$ and (*b*) the fundamental and second harmonic irradiances versus (normalized to L_{p}) distance for type II phase-matching for the strong fundamental I_1 (long-broken curve, along horizontal axis), the weak fundamental I_2 (short-broken curve) and the second harmonic (full curve) (from [24]).

three beams oscillates with distance instead of asymptotically approaching a constant which occurs for type I. Defining the irradiance imbalance as $\delta = [I_1(0) - I_2(0)]/[I_1(0) + I_2(0)]$ with $I_1(0) > I_2(0)$, the oscillation period shown in figure 6 is given by

$$L_{\mathrm{p}}(\delta) = \frac{2K[(1-\delta)/(1+\delta)]}{\sqrt{1+\delta}} \tag{17}$$

where K is a complete elliptical integral of the first kind [24].

The distance dependence of the nonlinear phase shifts can be understood in terms of the Manley–Rowe relations which require that equal energies be removed from both fundamental beams during SHG. The stronger beam can only be depleted to the point that the weaker beam is completely depleted. For the stronger beam to grow during the succeeding down-conversion cycle, the right-hand side of equation (14) requires a change in sign which can only be accomplished by $a_1(z)$ changing phase by π when its energy increases back from complete depletion. This explains the nonlinear phase shift behaviour for the weak fundamental shown in figure 6(b). Similarly, the harmonic phase must change by π when the fundamentals pass through a maximum and the harmonic is completely depleted. The stronger fundamental can never undergo a discontinuous phase change since it never completely depletes.

Away from phase-matching, both fundamental beams experience nonlinear phase shifts. The larger the irradiance imbalance δ, the larger the ratio of the weak-to-strong beam nonlinear phase shift as shown in figure 7 [29]. Similar to the type I case, the phase shifts become linear in the field $(a_1(0))$ at high irradiances, exhibiting apparent saturation in figure 7. The key feature, however, is that the weak-beam nonlinear phase shift is optimum when $\delta \to 1$, whereas the strong beam experiences a small phase shift. Therefore the 'cross-phase' modulation of the orthogonally polarized weak beam is large and the 'self-phase' modulation of the strong beam is small, a very unusual property for nonlinear optics. As $\delta \to 0$, the phase shift for the two fundamental beams becomes equal.

Nonlinear eigenmodes also exist for this case, as considered in detail by Kaplan [26].

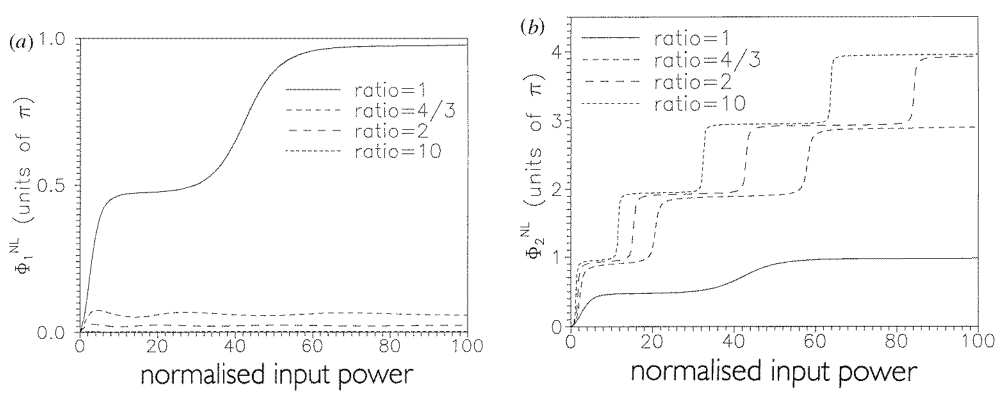

Figure 7. The nonlinear phase shift of $\phi^{\mathrm{NL}}(L)$ of the strong (a) and weak (b) fundamental input beams versus normalized input power for various ratios of $I_1(0)/I_2(0)$ at a phase mismatch of $\Delta kL = 0.1\pi$ (from [29]).

4. Cross-phase modulation

A key question is whether the equivalent of the familiar $\chi^{(3)}$-based cross-phase modulation is possible with cascading. Although always present with third-order nonlinearities, in cascading the beams must be coupled via appropriate $\chi^{(2)}$ coefficients and there must be energy exchange between them. By virtue of this coupling, cross-phase modulation occurs naturally between the fundamental(s) and the harmonic, as well as between all of the waves participating in sum and difference frequency generation of which type II SHG is a limiting case.

A different but probably rare form of cross-phase modulation is feasible with two orthogonally polarized fundamental inputs which are separately and independently linked to the same second harmonic via different $\chi^{(2)}$ tensor elements. That is, a second harmonic can be generated by either one of the fundamental beams alone. This would be difficult to implement in bulk crystals but is conceivable in waveguides. This case and some of its repercussions have been considered by Assanto and co-workers [30]. There are many variables, specifically the two effective nonlinearities, detunings, relative powers, etc. They found, for example, that if one of the fundamentals is weaker than the other, it is possible to control the strong-beam output just by varying the relative phase between the two inputs, i.e. the phase of the weak beam.

5. Experimental measurements of SHG-generated nonlinear phase shifts

The nonlinear phase shifts discussed above have been measured for both type I and II SHG, in both bulk crystals and waveguides.

5.1. Bulk crystals

As discussed in the introduction, the cascaded nonlinearity has, for many years, been inferred because it interferes with the usual third-order nonlinearities. The first direct measurement was by Belashenkov *et al* (1989) on bulk CDA [4]. More recently DeSalvo and co-workers using Z-scan measured the complete detuning and fundamental depletion curves near SHG phase-matching in KTP [5]. Their results are reproduced in figure 8. They realized that

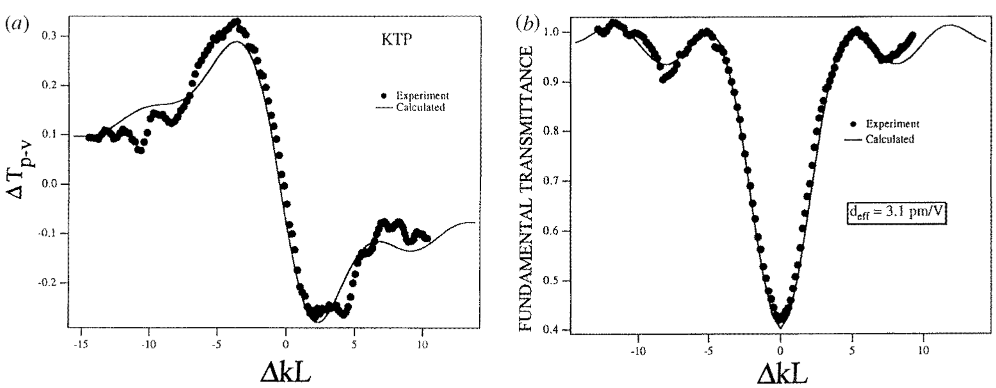

Figure 8. (a) The nonlinear phase shift $\phi^{\mathrm{NL}}(L)$ ($\propto \Delta T_{\mathrm{p\text{-}v}}$) versus detuning ΔkL for KTP measured at 1064 nm using Z-scan with an incident power of 9.4 GW cm^{-2} on focus. (b) The corresponding fundamental transmission (from [5]).

cascading was the dominant mechanism and the agreement with cascading theory was excellent. What is most noteworthy is that the cascading effect at its optimum detuning was much larger than the corresponding third-order nonlinearity in KTP.

One of the unique aspects of cascading is that the temporal response of the nonlinear phase shift is not necessarily given by the temporal response of $\chi^{(2)}$ which is ultrafast off-resonance. The response in fact depends on the detuning from another resonance, namely the SHG resonance. Figure 5(a) can be interpreted as a frequency detuning curve, showing that there is a limited bandwidth associated with cascading if used near phase-matching. The importance of this bandwidth depends on where the centre frequency of a pulse occurs. For large detunings, the change in the frequency response of the nonlinear phase shift is relatively slow with frequency and hence very short pulses can be used. The influence of the SH bandwidth becomes more severe for pulses near the phase-matching condition if the pulse bandwidth is broader than the phase-matching bandwidth. This effect has been observed for β-barium borate, and the corresponding calculations by Hache *et al* are shown in figure 9 [31]. These results show a significant decrease in the net nonlinear phase shift for pulses shorter than 300 fs in β-barium borate.

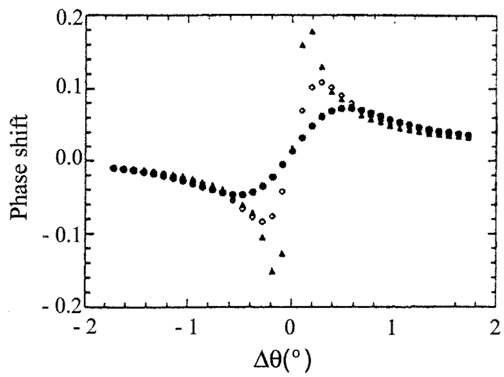

Figure 9. Calculated nonlinear phase shifts $\phi^{\mathrm{NL}}(L)$ versus angular detuning from phase match for 50 fs (full circles), 100 fs (open diamonds) and 300 fs (full triangles) pulses for constant peak input fundamental irradiance (from [31]).

The nonlinear phase shift has now been measured in a number of materials, primarily with the Z-scan technique. Some examples are $KNbO_3$, CDA, KTP and β-barium borate [4, 5, 32, 33]. Examples of single-crystal organics which have been measured are DAN and MBA-NP [34, 35]. To date, the largest effective nonlinearities reported have been of the order of 2×10^{-13} cm^2 W^{-1} obtained near phase-matching in a 0.8 mm thick DAN single crystal, a factor of five larger than CS_2 even for such a short crystal [34].

5.2. Waveguides

Applications requiring operation at small input power will probably require optical waveguides for successful implementation. Sundheimer *et al* used spectral broadening to deduce the phase shift in segmented, ion-exchanged KTP waveguides [36]. This was an indirect measurement which was complicated by the pulse distortion which occurs due to temporal pulse walk-off. The nonlinear phase shift was measured interferometrically in $LiNbO_3$ channel waveguides which utilized temperature-tuned type I phase-matching at 1320 nm [37]. The measured dependence of the nonlinear phase shift versus detuning

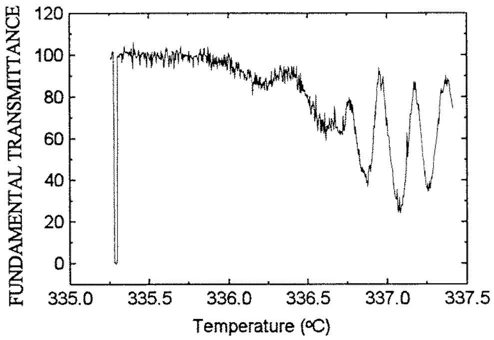

Figure 10. Fundamental transmission $P_\omega(L)/P_\omega(0)$ (in %) near type I phase-matching for SHG in $LiNbO_3$ channel waveguides versus temperature in the centre of the oven for temperature-tuned phase-matching $[(T - T_{PM}) \propto \Delta kL]$ (from [37]).

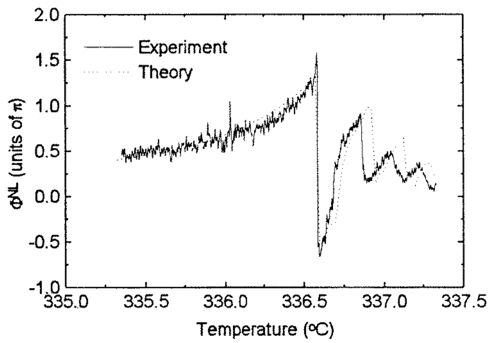

Figure 11. Nonlinear phase shift $\phi^{NL}(L)$ near type I phase-matching for SHG in $LiNbO_3$ channel waveguides versus temperature in the centre of the oven for temperature-tuned phase-matching (from [37]).

was radically different from that shown in, for example, figure 5. One aspect was that phase shifts of 1–2π were obtained with less than 10% conversion of the fundamental to the second harmonic. This was a direct consequence of the sample geometry and the wavevector mismatch distribution introduced by temperature gradients within the oven. Because of the short working distance of the lens required for coupling into the single-mode waveguides, the sample ends were located right at the oven windows where the temperature was lower than in the central part of the oven (and waveguide). Thus, when the central part of the waveguide was wavevector-matched, the ends were not, and vice versa. This led to a highly asymmetric fundamental throughput around the temperature (336.6 °C) associated with phase-matching the central part of the waveguide, as shown in figure 10. The nonlinear phase shift (figure 11) was measured directly with a Mach–Zehnder interferometer. The key point is that a large nonlinear phase shift ($> 1.5\pi$) was measured commensurate with a loss of only 10% or less to SHG at the output.

The results in figures 10 and 11 have very important repercussions. With a uniform wavevector mismatch along the waveguide and useful nonlinear phase shifts, the throughput of the fundamental is dramatically reduced due to SHG. These $LiNbO_3$ results showed that this loss to SHG can be minimized with an appropriate wavevector mismatch distribution with distance. The 'price' for minimizing this 'loss' is that the required waveguide length is increased relative to the uniform wavevector mismatch case.

Cascaded phase shifts have also been measured in a single-crystal core fibre using the organic DAN in the core [34]. Although the second harmonic was emitted in the form of Cerenkov radiation into the fibre glass cladding, cascaded phase shifts still occurred. A nonlinear phase shift of $\pi/4$ was obtained with only a few tens of Watts of input.

6. Summary

'Cascading' based on second-order nonlinearities does offer an alternative to achieving a number of effects normally associated with third-order nonlinear optics. Here we have specifically concentrated on the effective irradiance-dependent refractive index coefficient which is of interest for many applications. Although potentially the cascading effects can be much larger than their third-order counterparts, it is necessary to operate near the phase-matching condition for some parametric mixing process such as second harmonic generation. More effort needs to be put into this area, especially for organic crystals.

The characteristics of the nonlinear phase shifts generated via cascading are in many ways different from their third-order counterparts. Specifically, the phase shift increases in a stepwise fashion with a period given by the coherence length, even far from phase-matching where the steps are small. Only in certain irradiance and detuning ranges is the response linear in irradiance. For large phase shifts the response is linear in the fundamental field. Finally, cross-phase modulation is not easy to implement relative to the third-order nonlinear case.

Although not discussed in any detail here, a number of applications have already been demonstrated including all-optical switching, optical transistor action, mode-locking, pulse compression, soliton generation, etc, and more can be expected in the near future.

Acknowledgments

The author wishes to acknowledge and thank DARPA, ARO, NSF and AFOSR for supporting various aspects of the cascading research at CREOL.

References

[1] Ostrovskii L A 1967 Self-action of light in crystals *JETP Lett.* **5** 272–5

[2] Yablonovitch E, Flytzanis C and Bloembergen N 1972 Anisotropic interference of three-wave and double two-wave frequency mixing in GaAs *Phys. Rev. Lett.* **29** 865–8

Akhmanov S A, Dubovik A N, Saltiel S M, Tomov I V and Tunkin V G 1974 Nonlinear optical effects of fourth order in the field in a lithium formate crystal *JETP Lett.* **20** 117–8

Akhmanov S A, Dubovik A N, Saltiel S M, Tomov I V and Tunkin V G 1974 *Zh. Eksp. Teor. Fiz. Pis. Red.* **20** 264–8

[3] Flytzanis Chr and Bloembergen N 1976 Infrared dispersion of third-order susceptibilities in dielectrics: retardation effects *IEEE J. Quantum Electron.* **QE-4** 271–300

Flytzanis Chr 1975 *Quantum Electronics* vol 1, part A, ed H Rabin and C L Tang (New York: Academic)

[4] Belashenkov N R, Gagarskii S V and Inochkin M V 1989 Nonlinear refraction of light on second-harmonic generation *Opt. Spectrosc.* **66** 806–8

[5] DeSalvo R, Hagan D J, Sheik-Bahae M, Stegeman G and Van Stryland E W 1992 Self-focusing and self-defocusing by cascaded second-order effects in KTP *Opt. Lett.* **17** 28–30

[6] Cerullo A, De Silvestri S, Monguzzi A, Segala D and Magni V 1995 Self-starting mode locking of a cw Nd:YAG laser using cascaded second-order nonlinearities *Opt. Lett.* **20** 746–8

[7] Yamashita M, Torizuka K, Uemiya T and Shimada J 1991 Compression of nonamplified femtosecond pulses using nonlinear organic fibers *Appl. Phys. Lett.* **58** 2727–8

[8] Schiek R, Baek Y, Krijnen G, Stegeman G I, Baumann I and Sohler W 1996 All-optical switching in lithium niobate directional couplers with the cascaded nonlinearity *Opt. Lett.* **21** 940–2

[9] White A G, Mlynek J and Schiller S 1996 Cascaded second-order nonlinearity in an optical cavity *Europhys. Lett.* **35** 425–30

[10] Danelius R, Di Trapani P, Dubietis A, Piskarkas A and Podenas D 1993 Self-diffraction through cascaded second order frequency-mixing effects in β-barium borate *Opt. Lett.* **18** 574–6

[11] Hagan D J, Sheik-Bahae M, Wang Z, Stegeman G, Van Stryland E W and Assanto G 1994 Phase controlled transistor action by cascading of second-order nonlinearities in KTP *Opt. Lett.* **19** 1305–7

[12] Treviño-Palacios C G, Stegeman G I and Baldi P 1996 Spatial nonreciprocity in waveguide second order processes *Appl. Phys. Lett.* **21** 1442–4

[13] Gustafson T K, Taran J-P E, Kelley P L and Chiao R Y 1970 Self-modulation of picosecond pulses in electro-optic crystals *Opt. Commun.* **2** 17–21

[14] Bosshard Ch, Speiter R, Zgonik M and Gunter P 1995 Kerr nonlinearity via cascaded optical rectification and the linear electro-optic effect *Phys. Rev. Lett.* **74** 2816–9

[15] Zgonik M and Günter P 1996 Cascading nonlinearities in optical four wave mixing *J. Opt. Soc. Am.* B **13** 570–6

[16] Karamzin Yu N and Sukhorukov A P 1974 Nonlinear interaction of diffracted light beams in a medium with quadratic nonlinearity: mutual focusing of beams and limitation on the efficiency of optical frequency convertors *JETP Lett.* **20** 339–42

Karamzin Yu N and Sukhorukov A P 1975 Mutual focusing of high-power light beams in media with quadratic nonlinearity *Zh. Eksp. Teor. Fiz.* **68** 834–40 (Engl. transl. 1976 *Sov. Phys.–JETP* **41** 414–20)

[17] Torruellas W E, Wang Z, Hagan D J, Van Stryland E W, Stegeman G I, Torner L and Menyuk C R 1995 Observation of two-dimensional spatial solitary waves in a quadratic medium *Phys. Rev. Lett.* **74** 5036–9

[18] Notation taken from Hopf F A and Stegeman G I 1985 *Applied Classical Electrodynamics, Volume 2: Nonlinear Optics* (New York: Wiley)

[19] Lawrence B, Cha M, Kang J U, Torruellas W, Stegeman G I, Baker G, Meth J and Etemad S 1994 Large purely refractive nonlinear index of single crystal p-toluene sulfonate (PTS) at 1600 nm *Electron. Lett.* **30** 447–8

[20] For example, Laddies I, Lepers C, Périgaud A, Badan J and Zyss J 1990 Linear and nonlinear optical properties of N-4-nitrophenyl L-propinol single crystals *Opt. Commun.* **80** 149–54

[21] Levine B F, Bethea C G, Thurmond C D, Lynch R T and Bernstein J L 1979 An organic crystal with an exceptionally large optical second-harmonic coefficient: 2-methyl-4-nitrolaniline *J. Appl. Phys.* **50** 2523–7

[22] For example, Marder S R, Perry J W and Yakymyshyn C R 1994 Organic salts with large second order nonlinearities *Chem. Mater.* **6** 1137–47

Bosshard Ch, Sutter K, Schlesser R and Gunter P 1993 Electro-optic effects in molecular crystals *J. Opt. Soc. Am.* B **10** 867–85

[23] Armstrong J A, Bloembergen N, Ducuing J and Pershan P S 1962 Interaction between light waves in a nonlinear dielectric *Phys. Rev.* **127** 1918–39

[24] Kobyakov A, Peschel U, Muschall R, Assanto G, Torchigin V P and Lederer F 1995 Analytical approach to all-optical modulation by cascading *Opt. Lett.* **20** 1686–8

Kobyakov A, Peschel U and Lederer F 1996 Vectorial type-II interaction in cascaded quadratic nonlinearities—an analytical approach *Opt. Commun.* **124** 184–94

[25] Stegeman G I, Sheik-Bahae M, Van Stryland E W and Assanto G 1993 Large nonlinear phase-shifts in second-order nonlinear-optical processes *Opt. Lett.* **18** 13–5

[26] Trillo S, Wabnitz S, Chisari R and Cappellini G 1992 Two-wave mixing in a quadratic nonlinear medium: bifurcations, spatial instabilities, and chaos *Opt. Lett.* **17** 637–9

Kaplan A E 1993 Eigenmodes of $\chi^{(2)}$ wave mixings: cross-induced second-order nonlinear refraction *Opt. Lett.* **18** 1223–5

[27] Hutchings D, Aitchison J S and Ironside C N 1993 All-optical switching based on nondegenerate phase shifts from a cascaded second-order nonlinearity *Opt. Lett.* **18** 793–5

[28] Belostotsky A L, Leonov A S and Meleshko A V 1994 Nonlinear phase change in type II second-harmonic generation under exact phase-matched conditions *Opt. Lett.* **19** 856–8

[29] Assanto G, Torelli I and Trillo S 1994 All-optical processing by means of vectorial interactions in second-order cascading: novel approaches *Opt. Lett.* **19** 170–2

Assanto G 1995 Transistor action through nonlinear cascading in type II interactions *Opt. Lett.* **20** 1595–7

Assanto G and Torelli I 1995 Cascading effects in type II second harmonic generation: applications to all-optical processing *Opt. Commun.* **119** 143–8

[30] Assanto G, Torelli I and Trillo S 1994 All-optical phase controlled amplitude modulator *Electron. Lett.* **30** 733–5

[31] Hache F, Zéboulon A, Gallot G and Gale G M 1995 Cascaded second-order effects in the femtosecond regime in β-barium borate: self-compression in visible optical parametric oscillator *Opt. Lett.* **20** 1995–8

[32] Tan H, Banfi G P and Tomaselli A 1993 Optical frequency mixing through cascaded second-order processes in β-barium borate *Appl. Phys. Lett.* **63** 2472–5

[33] Desalvo J R 1993 On nonlinear refraction and two-photon absorption in optical media *PhD Thesis* University of Central Florida, ch 7

[34] Kim D Y, Torruellas W E, Kang J, Bosshard C, Stegeman G I, Vidakovic P, Zyss J, Moerner W E, Twieg R and Bjorklund G 1994 Second-order cascading as the origin of large third-order effects in organic single-crystal-core fibers *Opt. Lett.* **19** 868–70

[35] Nitti S, Tan H M, Banfi G P and Degiorgio V 1994 Induced 'third-order' nonlinearity via cascaded second-order effects in organic crystals of MBA-NP *Opt. Commun.* **106** 263–8

[36] Sundheimer M I, Bosshard Ch, Van Stryland E W, Stegeman G I and Bierlein J D 1993 Large nonlinear phase modulation in quasi-phasematched KTP waveguides due to cascaded second-order processes *Opt. Lett.* **18** 1397–9

Sundheimer M L, Villeneuve A, Stegeman G I and Bierlein J D 1994 Cascading nonlinearities in KTP waveguides at communications wavelengths *Electron. Lett.* **30** 1401–2

[37] Schiek R, Sundheimer M L, Kim D Y, Baek Y, Stegeman G I, Suche H and Sohler W 1994 Direct measurement of cascaded nonlinearity in lithium niobate channel waveguides *Opt. Lett.* **19** 1949–51